Cell Imaging Hot Paper

Deutsche Ausgabe: DOI: 10.1002/ange.201507281
Internationale Ausgabe: DOI: 10.1002/anie.201507281

The *cis*-Diammineplatinum(II) Complex of Curcumin: A Dual Action DNA Crosslinking and Photochemotherapeutic Agent

Koushambi Mitra, Srishti Gautam, Paturu Kondaiah, and Akhil R. Chakravarty**

Dedicated to Professor Animesh Chakravorty on the occasion of his 80th birthday

Abstract: *[Pt(cur)$(NH_3)_2$](NO_3) (**1**), a curcumin-bound cis-diammineplatinum(II) complex, nicknamed Platicur, as a novel photoactivated chemotherapeutic agent releases photoactive curcumin and an active platinum(II) species upon irradiation with visible light. The hydrolytic instability of free curcumin reduces upon binding to platinum(II). Interactions of **1** with 5′-GMP and ct-DNA indicated formation of platinum-bound DNA adducts upon exposure to visible light ($\lambda = 400$–700 nm). It showed apoptotic photocytotoxicity in cancer cells ($IC_{50} \approx 15$ μM), thus forming $^{\cdot}OH$, while remaining passive in the darkness ($IC_{50} > 200$ μM). A comet assay and platinum estimation suggest Pt–DNA crosslink formation. The fluorescence microscopic images showed cytosolic localization of curcumin, thus implying possibility of dual action as a chemo- and phototherapeutic agent.*

The therapeutic pathway of cisplatin involves dissociation of the Pt–Cl bonds to form a diaquadiammineplatinum(II) species which acts as a transcription inhibitor by forming platinum–nuclear DNA crosslinks and triggers apoptosis, thus eventually leading to cellular senescence.[1] Modulation of the kinetic processes involved has led to the introduction of cisplatin analogues such as carboplatin and oxaliplatin. These platinum(II) species together are considered the backbone of cancer chemotherapy. The potency of platinum-based anticancer agents is limited by several undesired side-effects, such as nephrotoxicity, hepatotoxicity, neurotoxicity, and ototoxicity, as well as the drug-resistance of cisplatin.[1c] A new strategy has emerged in which six-coordinate Pt^{IV} complexes, as inert prodrugs, are shown to release four-coordinate active platinum(II) species upon reduction by cellular glutathione or upon photoactivation.[2] The Pt^{IV} diazido complexes in blue light show remarkable cytotoxicity.[3] Photoactivated chemotherapy (PACT) as a complementary methodology to photodynamic therapy (PDT) has emerged as a viable modality for cancer treatment in which a prodrug showing lower or even no dark toxicity is photoactivated to generate cytotoxins selectively within the cancerous tissues.[4] The control of the drug release and drug doses makes PDT more advantageous in contrast to the conventional anticancer therapies.[5,6]

To circumvent two major predicaments associated with cisplatin, that is 1) the nuclear excision repair mechanism and 2) rapid dissociation of the chlorides, one needs to consider different sets of ligands instead of chloride. The use of O,O-donor ligands, such as oxalic acid in oxaliplatin or a dicarboxylic acid in carboplatin, has shown improvement in the efficacy of the drug.[1] Another alternate and viable strategy could be to direct the platinum(II) complex to mitochondrial DNA instead of nuclear DNA. We put forward a new strategy in this communication in which a different class of O,O-donor ligand, well known for showing preferential cytosolic localization than nuclear uptake, is used in designing a cisplatin analogue. The O,O-donor ligand is curcumin (Hcur), which in its enolic form binds to metals. Hcur is derived from yellow turmeric and has diverse medicinal properties as a traditional Indian and Chinese medicine. Curcumin itself has the ability to inhibit various proinflammatory transcription factors (NF-κB), thus leading to its remarkable anti-inflammatory and anticancer properties.[7] Despite immense potency and safety at high doses, it has failed to gain much approval as a therapeutic agent because of its low aqueous solubility, rapid metabolism leading to degradation, and reduced bioavailability (only 1% of actual dose retained in plasma of rats after 1 h of oral administration).[8] Reports have shown that the degradation of curcumin can be arrested upon its complexation with d- and f-block metal ions.[9] Curcumin has an intense absorption band in the visible region at about $\lambda =$ 430 nm and this imparts its photosensitizing abilities. The triplet state of photoactivated curcumin reacts with molecular oxygen and generates reactive oxygen species (ROS). Moreover, the green emissive band of the dye at about $\lambda = 520$ nm enables cellular imaging and tracking of its conjugates within the cell.

With an objective to achieve controlled cellular delivery of curcumin, we have designed and synthesized a platinum(II) complex of curcumin, [Pt(cur)$(NH_3)_2$](NO_3) (**1**). The complex **1**, called Platicur, is found to release curcumin and a cisplatin analogue upon irradiation with visible light ($\lambda = 400$–700 nm). Light activation imparts controlled release of curcumin. Though curcumin has earlier been used as an adjuvant and in combination with cisplatin for cancer treatment,[10] no previous attempt is documented involving the delivery of both curcumin and a cisplatin analogue from a single prodrug. The complex **1** and its acetylacetonate analogue [Pt(acac)-

[*] K. Mitra, Prof. A. R. Chakravarty
Department of Inorganic and Physical Chemistry
Indian Institute of Science
Bangalore 560012, Karnataka (India)
E-mail: arc@ipc.iisc.ernet.in
S. Gautam, Prof. P. Kondaiah
Department of Molecular Reproduction, Development and Genetics,
Indian Institute of Science
Bangalore 560012, Karnataka (India)
E-mail: paturu@mrdg.iisc.ernet.in

Supporting information for this article is available on the WWW under http://dx.doi.org/10.1002/anie.201507281.

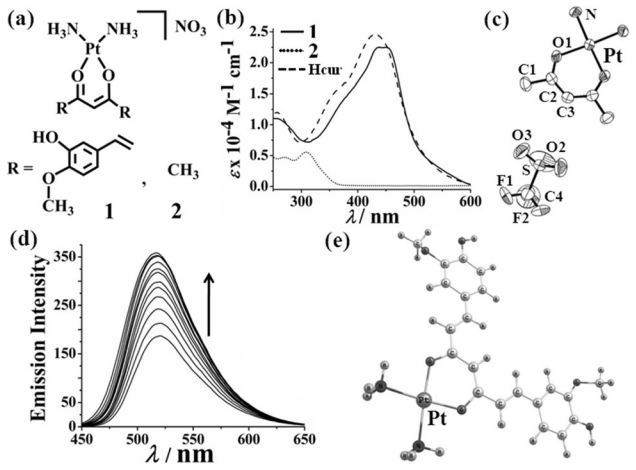

Figure 1. a) Chemical structures of **1** and **2**. b) UV-visible spectra of **1**, **2**, and Hcur (100 μM) in 10% DMSO/DPBS (pH 7.2). c) ORTEP drawing of **2a**.[11] Thermal ellipsoids shown 50% probability. H atoms are omitted for clarity. d) Increase in emission intensity of **1** (50 μM in 1:1 DMSO/water), monitored at $\lambda = 530$ nm ($\lambda_{exc} = 430$ nm), upon photoirradiation (visible light, $\lambda = 400$–700 nm). Data recorded at 10 min time intervals. e) Energy-minimized structure of **1** using B3LYP/LanL2DZ (for Pt)/6-31 + G (for other atoms) level of theory.

$(NH_3)_2](NO_3)$ (**2**), as a control, were synthesized in about 70% yield upon reacting cisplatin with $AgNO_3$, with subsequent addition of curcumin (Hcur) for **1** and acetylacetone (Hacac) for **2** in the presence of a base (Figure 1a; see Scheme S1 in the Supporting Information). The complexes are characterized by ESI-MS, NMR, HPLC, ICP-MS, IR, CHN, redox, and electronic spectral data (see Figures S1–S6 and Table S1). The molar conductance value of about 80 $S\,cm^2\,mol^{-1}$ in aq. DMF (1:1 v/v) at 25°C suggests 1:1 electrolytic nature of the complexes. A single peak in the mass spectra corresponding to $[M-NO_3]^+$ species (*m*/*z* 596.13 for **1** and 328.05 for **2**) indicated formation of the desired complexes. The isotopic distribution further confirmed the presence of platinum in the ionic form (see Figure S1). The ^{1}H NMR spectrum of **1** showed the γ-proton of the diketone moiety having an up-field shift of 0.1 ppm as compared to that in Hcur. The IR spectra showed characteristic peaks at 3200 ($\nu_{N\text{-}H}$), 1590 ($\nu_{C=O}$), and 1495 ($\nu_{C=C}$) cm^{-1}. The complex **1** (1 mM in DMF-0.1M TBAP) showed an irreversible response at −1.35 V versus SCE, and is characteristic of curcumin [E_f(Hcur) = −1.80 V] (see Figure S4c,d). The absence of any metal-based redox activity indicates the electrochemical stability of the complex. The solution purity of the complexes (ca. 95%) was ascertained using ICP-MS and HPLC methods (see Figure S5), and in the solid state by CHN analysis. The absorption spectra of **1** (100 μM) in 10% DMSO/DPBS (pH 7.2) exhibited two equally intense bands at $\lambda = 460$ and 435 nm ($\varepsilon = 22\,500\ M^{-1}\,cm^{-1}$) with a shoulder at $\lambda = 385$ nm ($\varepsilon = 15\,000\ M^{-1}\,cm^{-1}$; Figure 1b). The acac complex **2** ($\lambda_{max} = 308$ nm) did not show such bands. The complex **1** was emissive ($\lambda_{em} = 530$ nm) when excited at $\lambda = 430$ nm, thus giving a quantum yield (Φ) value of 0.02 in 1:1 aq. DMSO (Φ of curcumin, 0.04; see Figure S6a). The complex **2** as its CF_3SO_3 salt (**2a**) was structurally characterized by X-ray crystallography (Figure 1c; see Tables S2 and S3 and Figure S6b).[11] The complex crystallized in the orthorhombic $Cmc2_1$ space group and has the Pt^{II} center in a distorted square-planar geometry with two ammine ligands and a chelating monoanionic acac. The Pt–O and Pt–N bond lengths are 1.990(6) and 2.046(8) Å, respectively.

The stability of **1** and **2** were studied in 10% DMSO/DPBS or DMEM (pH 7.2, 37°C) by monitoring UV-visible spectral changes with time. The complex **1** showed slow hydrolysis (initial rate, $k_{hyd} = 8.9 \times 10^{-7}\ min^{-1}$ for **1**). The dye alone degraded rapidly and only about 10% remained intact after 4 hours, while **1** was about 75% intact (see Figure S7). This data indicates enhanced stability of the β-diketone moiety upon complex formation. There was no noticeable change in the ^{1}H NMR spectra in 1:1 D_2O/[D_4]MeOH, even after 48 hours, and thus further suggested the stability of the complexes. Platinum analogues having O,O-donor ligands are known for slow release of the ligands in a cellular medium. Photorelease of these ligands from the platinum(II) center is known.[12] The excellent photophysical properties of curcumin and the 5d Pt^{II} heavy metal amplify the possibilities of such phototriggered conversions of **1**. Thus we studied the possibility of release of the dye upon exposure to light (Luzchem; $\lambda = 400$–700 nm) and in the dark. The emission intensity of free curcumin is dampened in the metal-bound form (see Figure S6a). An increment in emission intensity therefore will indicate the release of curcumin. We observed this enhancement of emission intensity at $\lambda = 530$ nm upon photoexposure of **1** (Figure 1d). However, the intensity remained unaltered in the darkness for 24 hours, thus indicating the importance of light activation for metal–O,O-donor ligand bond dissociation (see Figure S8).

The fluorescence lifetimes were measured to support our hypothesis. The respective values in 1:1 aqueous DMSO in the dark are 13.6 and 23 ps for **1** and curcumin. The solutions of **1** after 1 hour of light exposure gave a lifetime of 19.4 ps, which is similar to that of free curcumin (see Table S4). It remained unaltered for curcumin when exposed to light. The absorption spectra of **1** showed a decrease in the intensity at $\lambda = 460$ and 435 nm upon light exposure with concomitant increase at $\lambda = 385$ nm and the appearance of a band at $\lambda =$ 400 nm (see Figure S8d). These bands are assignable to curcumin and its degraded products.[13] The experiments in 10% DMSO/DPBS showed a rapid loss of the emission and absorption intensity (initial rate of photodegradation, $k_{photo} = 2.8 \times 10^{-6}\ min^{-1}$) upon photoexposure for 10 minutes ($\lambda =$ 400–700 nm), owing to the instability of the released curcumin at pH 7.2 (see Figure S9). The mass spectral analysis of the irradiated samples of **1** confirmed the presence of free curcumin (*m*/*z* 369, $[M+H]^+$) and its hydrolyzed products (see Figure S10). Loss of curcumin from the platinum(II) center is expected to form an aqua species capable of forming crosslinks with DNA. To evaluate such a possibility, **1** was mixed with guanosine monophosphate (5′-GMP, 1:10 ratio in 1:1 D_2O/[D_6]DMSO) and ^{1}H NMR spectra were recorded after 8 hours of light exposure ($\lambda = 400$–700 nm) and showed the appearance of new peaks at $\delta = 8.5$ and 9.2 ppm (see Figure S11). The H8 proton of uncoordinated 5′-GMP appeared at $\delta = 8.1$ ppm. This proton experienced downfield

shift upon coordination of 5′-GMP to Pt at N7, and is characteristic of the Pt–GMP adducts.[14] The downfield shift of $\delta = 0.4$ and 1.1 ppm can be respectively assigned to the bi- and monofunctional adduct. The bifunctional adduct was detected in the mass spectra ($m/z = 477.08$; see Figure S12a). In contrast, **1** reacts with 5′-GMP in the dark only after 30 hours. The DNA crosslink formation was also evidenced from the experiments using ct-DNA (300 μM) and ethidium bromide (EB, 50 μM) in 5% DMSO/DPBS medium. EB, upon intercalation within DNA, increases its emission intensity as a result of entrapment in the hydrophobic core. Upon treatment with the complex (50 μM) and light, the emission intensity of DNA-intercalated EB decreased (ca. 13%) at $\lambda =$ 595 nm ($\lambda_{exc} = 546$ nm), thus suggesting formation of Pt–DNA adducts (see Figure S12b). Thiourea (10 mM) treatment led to a marginal increase in its emission intensity, thus indicating that about 2% of adducts were monofunctional. Curcumin alone did not alter the emission intensity of EB. To rule out any displacement of EB by **1** with DNA, the DNA melting studies were performed. The complex **1** and curcumin showed no DNA intercalative property ($\Delta T_m \approx 0$ °C) as compared to EB ($\Delta T_m \approx 19$ °C; see Figure S13a). Interestingly, **1**, upon light exposure, gave similar temperature shifts to those of cisplatin in the dark ($\Delta T_m \approx 1.0$ °C). The complex was stable at 100 °C, thus ensuring no thermal degradation of **1** during the DNA melting studies. Viscosity studies revealed non-intercalative nature of **1** (see Figure S13b). Furthermore, an increased amount of Pt of about 170 ppb was detected by ICP-MS in light-exposed samples of **1** (100 μM) and ct-DNA (200 μM) [5% DMSO/DPBS buffer, pH 7.2] compared to samples incubated in the dark (see Figure S13c). The control complex **2** showed its photostability with no apparent formation of Pt–DNA adducts (see Figure S7d).

Theoretical calculations (B3LYP functional with basis sets LanL2DZ for Pt/6-31 + G* for C,H,N,O) were done to study the photophysical properties of **1**.[15] The $\lambda = 493$ nm ($f =$ 0.833) transition is assigned to the dissociative ^{1}LMCT: HOMO (Hcur)→LUMO (Pt–O bond; Figure 1e; see Tables S5 and S6). These are σ* towards Pt–O bonds, thus suggesting photocleavage. Pt promotes intersystem crossing (ISC) by spin-orbit coupling resulting in long-lived triplet states. The optimization of the triplet excited state geometry revealed elongation of the Pt–O bonds by about 0.2 Å with loss of planarity of the curcumin moiety (C1-C2-C3-C4 dihedral angle of 26°), thus suggesting the possibility of elimination of curcumin from the photoexcited state (see Figure S14a and Table S7). Concomitant loss of respective Mulliken charges on Pt and O was also observed in the excited state.

The photorelease of curcumin leading to the formation of a DNA crosslinking agent prompted us to assess the light-activated anticancer potency of **1**. The IC_{50} values were determined from the MTT assay in HaCaT (immortalized transformed skin keratinocytes), BT474 and T47D (breast epithelial ductal carcinoma), and Hep3B (hepatocarcinoma) cells (Figure 2; see Figure S15 and Table S8). The complex **1** gave IC_{50} values of 12–18 μM (4 h pre-incubation, 400–700 nm, 10 J cm^{-2}), and were nontoxic in the dark [$IC_{50} >$ 200 μM]. The IC_{50} values of **1** in light were comparable to

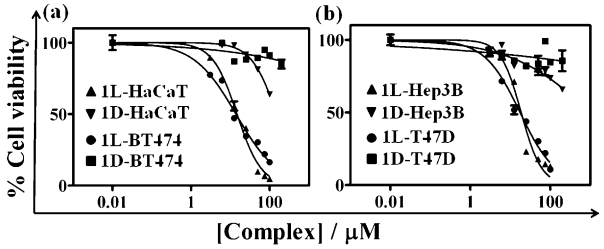

Figure 2. Cell viability plots of **1** for a) HaCaT and BT474 and b) Hep3B and T47D. There was a 4 h pre-incubation followed by either light exposure (L, $\lambda = 400$–700 nm, 10 J cm^{-2}) or without irradiation (D, in the dark).

that of free curcumin (10–13 μM). The acac complex **2** did not show any PDT activity. The complex **1** showed about a twofold lower photocytotoxicity [IC_{50}(light) ≈ 30 μM] in the immortalized nontransformed human peripheral lung epithelial HPL1D cells as compared to the cancer cells (see Figure S15 and Table S8). Since PDT is applicable to superficially exposed cells, we used HaCaT cells for further studies. The DCFDA assay, a quantitative method to assess cellular ROS formation, showed that about 90% of the HaCaT cells treated with **1** caused DCF formation only upon light exposure (Figure 3a; see Figure S16). AnnexinV/FITC-PI assay

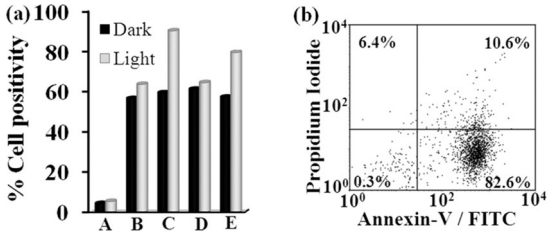

Figure 3. a) The percent cell positivity from a DCFDA assay for HaCaT cells upon 4 h pre-treatment with the compounds [A: cells alone; B: cells + DCFDA; C: **1** (18 μM); D: **2** (40 μM); E: curcumin (12 μM)] and 1 h light exposure ($\lambda = 400$–700 nm). b) AnnexinV-FITC/PI assay in HaCaT cells with **1** (18 μM, 4 h incubation, 1 h light-exposure) showing % apoptotic cell death [Quadrants: lower left = live cells, lower right = early apoptotic cells, upper right = late apoptotic cells, upper left = necrotic/dead cells].

revealed that about 83% of the total cell population of HaCaT cells treated with **1** (18 μM) was early apoptotic on light treatment while only 13% cell death was observed in the dark (Figure 3b; see Figure S17). The PI (propidium iodide) cell cycle analysis resulted in light-triggered arrest (ca. 58%) in the sub-G1 phase of **1**-treated HaCaT cells (see Figure S18). To understand the nature of ROS, we performed DNA photocleavage experiments using an Ar-Kr mixed gas ion laser (power = 50 mW) of $\lambda = 457$ nm (see Figure S19). The complex **1** (10 μM in buffer having 10% DMF) showed photocleavage of pUC19 DNA, thus forming about 90% of the nicked circular (NC) form. The presence of singlet-oxygen quenchers like NaN_3 and TEMP diminished the amount of the NC form by about 10%. However, addition of KI and DMSO as hydroxyl radical scavengers brought marked reduction (ca. 50% NC) in the DNA photocleavage activity,

thus suggesting that hydroxyl radicals are the major ROS. The DNA cleavage was also reduced (ca. 20% NC) under an inert atmosphere, thereby implying the need for aerial O_2 for its photoactivity.

Fluorescence microscopic images show cytoplasmic localization of **1** (20 μM) in HaCaT cells (Figure 4). This localization is important since it asserts direct damage on cellular metabolism and compels the cell to collapse.[16] The complex was located even after 4 hours, thus suggesting its stability, while free curcumin degraded with no apparent fluorescence after 2 hours (see Figure S20). Experiments were done to explore any release of curcumin in the cell upon treatment with light. The observed fluorescence enhancement indicated curcumin release (see Figure S21). Pt estimation in isolated nuclear and cytoplasmic fractions, by ICP-MS, confirmed that **1** (50 μM) remained in the cytoplasm in the dark (2.1 μg/10^6 cells; see Table S9). The experiment for exposure to light for 1 hour resulted in a substantial platinum content in both nuclear (1.68 μg/10^6 cells) and cytoplasmic (1.46 μg/10^6 cells) extracts. Moreover, **1** showed higher cellular uptake than either **2** or cisplatin because of the lipophilicity of curcumin. To examine formation of Pt–DNA crosslinks upon irradiation, the comet assay was performed in HaCaT cells. The complex (15 μM) showed only about 30% DNA content (untreated cells showing ca. 90%) in the tail region of the photoexposed cells, similar to that of cisplatin (200 μM in the dark), thus indicating Pt–DNA crosslink formation (see Figures S22 and S23).

In summary, we have been successful in delivering two anticancer agents, that is, curcumin and a cisplatin analogue, from a single prodrug, $[Pt(cur)(NH_3)_2](NO_3)$ (**1**), within the cancer cells upon light activation. The curcumin dye alone fails to reach the target tumour cells because of its hydrolytic instability in a buffer medium and poor bioavailability, while the nonspecific interaction of cisplatin results from its rapid uncontrolled hydrolysis. These drawbacks limit the medicinal applications of both curcumin and cisplatin. The observed in vitro photodegradation of **1**, from fluorescence studies and platinum estimations, is unique and unprecedented, thus permitting controlled generation of diammineplatinum(II) species as a DNA crosslinking/transcription inhibitor agent and the released curcumin as a PDT agent, in visible light, at the site of action. The remarkable phototoxic behavior of **1** in cancer cells ($IC_{50} \approx 12$–18 μM, 400–700 nm), along with the 15-fold lower toxicity in the dark, defines a new generation of visible-light activated dual-action anticancer agents.

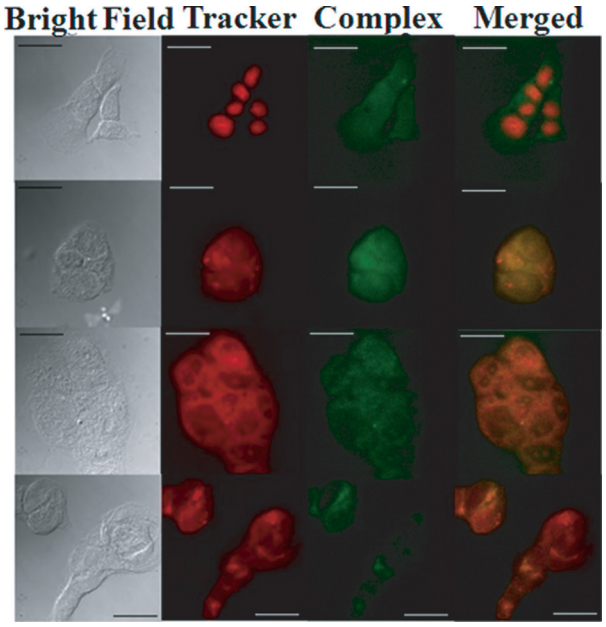

Figure 4. Fluorescence images of HaCaT cells upon 4 h incubation with **1** (20 μM), thus showing co-localization in ER. Trackers in rows 1 through 4: PI, MTR, ER-Tracker red, and lyso tracker red, respectively. Scale bar = 20 μm.

Acknowledgements

We thank the Department of Science and Technology (DST), Government of India, for financial support (SR/S5/MBD-02/2015), and the Alexander von Humboldt Foundation (Germany) for an electrochemical system. A.R.C. thanks DST for a J. C. Bose Fellowship. We thank Dr. R. Chakrabarti, Center of Earth Sciences, IISc for the ICP-MS facility.

Keywords: antitumor agents · cell imaging · curcumin · DNA · platinum

How to cite: *Angew. Chem. Int. Ed.* **2015**, *54*, 13989–13993
Angew. Chem. **2015**, *127*, 14195–14199

[1] a) E. Shaili, *Sci. Prog.* **2014**, *97*, 20–40; b) T. C. Johnstone, G. Y. Park, S. J. Lippard, *Anticancer Res.* **2014**, *34*, 471–476; c) A. M. Florea, D. Büsselberg, *Cancers* **2011**, *3*, 1351–1371.
[2] a) N. Graf, S. J. Lippard, *Adv. Drug Delivery Rev.* **2012**, *64*, 993–1004; b) R. K. Pathak, S. Marrache, J. H. Choi, T. B. Berding, S. Dhar, *Angew. Chem. Int. Ed.* **2014**, *53*, 1963–1967; *Angew. Chem.* **2014**, *126*, 1994–1998; c) E. Gabano, M. Ravera, D. Osella, *Dalton Trans.* **2014**, *43*, 9813–9820.
[3] a) Y. Zhao, N. J. Farrer, H. Li, J. S. Butler, R. J. McQuitty, A. Habtemariam, F. Wang, P. J. Sadler, *Angew. Chem. Int. Ed.* **2013**, *52*, 13633–13637; *Angew. Chem.* **2013**, *125*, 13878–13882; b) J. S. Butler, J. A. Woods, N. J. Farrer, M. E. Newton, P. J. Sadler, *J. Am. Chem. Soc.* **2012**, *134*, 16508–16511.
[4] M. Ethirajan, Y. Chen, P. Joshi, R. K. Pandey, *Chem. Soc. Rev.* **2011**, *40*, 340–362.
[5] W. A. Velema, W. Szymanski, B. L. Feringa, *J. Am. Chem. Soc.* **2014**, *136*, 2178–2191.
[6] a) R. N. Garner, J. C. Gallucci, K. R. Dunbar, C. Turro, *Inorg. Chem.* **2011**, *50*, 9213–9215; b) M. A. Sgambellone, A. David, R. N. Garner, K. R. Dunbar, C. Turro, *J. Am. Chem. Soc.* **2013**, *135*, 11274–11282.
[7] a) T. Esatbeyoglu, P. Huebbe, I. M. A. Ernst, D. Chin, A. E. Wagner, G. Rimbach, *Angew. Chem. Int. Ed.* **2012**, *51*, 5308–5332; *Angew. Chem.* **2012**, *124*, 5402–5427; b) M. Salem, S. Rohani, E. R. Gillies, *RSC Adv.* **2014**, *4*, 10815–10829.
[8] S. Prasad, A. K. Tyagi, B. B. Aggarwal, *Cancer Res. Treat.* **2014**, *46*, 2–18.
[9] a) S. Banerjee, A. R. Chakravarty, *Acc. Chem. Res.* **2015**, *48*, 2075–2083; b) A. K. Renfrew, N. S. Bryce, T. W. Hambley, *Chem. Sci.* **2013**, *4*, 3731–3739.

[10] W. Scarano, P. de Souza, M. H. Stenzel, *Biomater. Sci.* **2015**, *3*, 163 – 174.
[11] 1415424CCDC contains the supplementary crystallographic data for this paper. These data can be obtained free of charge from The Cambridge Crystallographic Data Centre.
[12] a) K. L. Ciesienski, L. M. Hyman, D. T. Yang, K. L. Haas, M. G. Dickens, R. J. Holbrook, K. J. Franz, *Eur. J. Inorg. Chem.* **2010**, 2224 – 2228; b) J. Mlcouskova, J. Stepankova, V. Brabec, *J. Biol. Inorg. Chem.* **2012**, *17*, 891 – 898; c) Y. Zhao, G. M. Roberts, S. E. Greenough, N. J. Farrer, M. J. Paterson, W. H. Powell, V. G. Stavros, P. J. Sadler, *Angew. Chem. Int. Ed.* **2012**, *51*, 11263 – 11266; *Angew. Chem.* **2012**, *124*, 11425 – 11428; d) K. Mitra, S. Patil, P. Kondaiah, A. R. Chakravarty, *Inorg. Chem.* **2015**, *54*, 253 – 264.
[13] U. Singh, S. Verma, H. N. Ghosh, M. C. Rath, K. I. Priyadarsini, A. Sharma, K. K. Pushpa, S. K. Sarkar, T. Mukherjee, *J. Mol. Catal. A* **2010**, *318*, 106 – 111.
[14] a) A. T. M. Marcelis, C. G. van Kralingen, J. Reedijk, *J. Inorg. Biol. Chem.* **1980**, *13*, 213 – 222; b) T. N. Singh, C. Turro, *Inorg. Chem.* **2004**, *43*, 7260 – 7262.
[15] A. D. Becke, *Phys. Rev. A* **1988**, *38*, 3098 – 3100 (see the Supporting Information for other references).
[16] Y. Zhao, E. B. Butler, M. Tan, *Cell Death Dis.* **2013**, *4*, e532.

Received: August 5, 2015
Revised: August 19, 2015
Published online: September 30, 2015

